Nambu-Goto string in QCD: Dipole interactions, scattering, and entanglement

Yizhuang Liu[*]
Institute of Theoretical Physics, Jagiellonian University, 30-348 Kraków, Poland

Maciej A. Nowak[†]
Institute of Theoretical Physics and Mark Kac Center for Complex Systems Research, Jagiellonian University, 30-348 Kraków, Poland

Ismail Zahed[‡]
Center for Nuclear Theory, Department of Physics and Astronomy, Stony Brook University, Stony Brook, New York 11794-3800, USA

(Received 28 July 2023; accepted 23 October 2023; published 16 November 2023)

We revisit some aspects of the stringy approach to dipole-dipole interactions, scattering and entanglement in QCD, using the Nambu-Goto (NG) string, without recourse to holography. We first show that the potential between two static dipoles exchanging closed NG strings is attractive at all separations. Underlining the exchange there is an emergent entropy, that is dominated by the tachyon at large separation, and vanishes at short separation, a measure of the confinement-deconfinement transition. The same tachyon is dominant in the scattering amplitude, as a correlator of two Wilson loops for two fixed dipolelike hadrons separated at large rapidity gap, where the contribution of the world sheet fermions is included. While the tachyon causes the mean string bit density to grow exponentially with the rapidity, the total scattering cross section still satisfies the Froissart bound by quantum shadowing. The stringy scattering exchange also carries an entanglement entropy, that saturates when the bound is reached. For hadrons with varying dipole sizes, the tachyon exchange takes place in hyperbolic space in the conformal limit. The result for the full S-matrix is reminiscent of the one from Mueller's evolved dipole wave function, for the total dipole-dipole cross section in perturbative QCD.

DOI: 10.1103/PhysRevD.108.094025

I. INTRODUCTION

String theory has been hailed as a possible consistent theory of quantum gravity. By pertinent compactifications, it has the potential to lead to various extensions of the standard model at higher energies. But perhaps the most compelling application of string theory may still be in strong interactions, where it originated from. It is plausible that QCD in the large number of colors N_c limit, may be dual to an effective string theory with a weak string coupling $g_s \sim \frac{1}{N_c}$, as suggested by holography in higher dimensions [1] (and references therein).

In so far, the compelling arguments for a QCD string stem from lattice QCD simulations [2] (and references therein). Indeed, detailed QCD lattice simulations in $1+2$ dimensions have shown that the closed flux tube in gauge theories with various N_c, are well described by a Nambu-Goto (NG) string in flat space dimensions [3]. Detailed studies of the string mass on its length for various N_c, yield results that are in good agreement with the NG string even for short lengths, well-beyond the contribution of the Luscher term. Although fuzzy, the string is well-approximated by a fundamental NG string. The extension of the lattice analysis to $(1+3)$-dimensions for $N_c = 3, 5$ for the closed string spectrum, has also shown convincing agreement with the NG string [4].

The description of the heavy quark-antiquark potential for fixed separation R, using a fully quantized NG string in $2+\mathrm{D}_\perp$-dimensions, was carried by Arvis with the result [5]

$$V(R) = \left(\sigma_T^2 R^2 - \frac{D_\perp}{24\alpha'}\right)^{\frac{1}{2}},$$

with the string tension $\sigma_T = 1/2\pi\alpha'$ and $\alpha' = l_s^2$. The large distance expansion of the NG potential, yields

[*]yizhuang.liu@uj.edu.pl
[†]maciej.a.nowak@uj.edu.pl
[‡]ismail.zahed@stonybrook.edu

$$V(R) \approx \sigma_T R - \frac{\pi D_\perp}{24R} - \frac{\pi^2}{2\sigma_T R^3}\left(\frac{D_\perp}{24}\right)^2, \tag{1}$$

the linear confining potential, plus the universal Luscher correction [6] and the Luscher-Weisz correction [7]. These three contributions are well-reproduced by the high-precision QCD lattice analysis of the interquark potential in [8]. Yet, the full NG potential becomes imaginary below a critical distance

$$R_c = \pi\sqrt{\frac{D_\perp \alpha'}{6}} = \frac{1}{2}\frac{|M_0|}{\sigma_T} \to \frac{1}{3}\ \text{fm}.$$

The rightmost numerical estimate following from $D_\perp = 2$, with $\alpha' = 1/2m_\rho^2$ the Regge rho meson slope. This behavior is tied to the tachyon with negative squared mass $M_0^2 < 0$ in the dual spectrum, and doomed the NG string as a fundamental string in 4-dimensions. Yet the tachyon mass is also at the origin of the measured large distance $1/R$ and $1/R^3$ corrections exhibited by the QCD string, which is fuzzy and not fundamental. The interquark potential below the critical R_c in QCD, is nonconfining. The lattice results [8,9] (see Figs. 1–3 therein) set the deviations at small separations $r < r_0$, with the Sommer scale $r_0 \sim 0.5$ fm. Hence, the use of the NG string to model QCD interactions, should prove useful away from criticality, for separations $r > r_0 > R_c$. The additional corrections to the NG string stemming from the constraints of Lorentz symmetry [10] are observed to be small in this range. In a way, this is consistent with the empirical success of the Cornell potential for charmonia [11]. In what follows, we will make use of these observations.

More specifically, we will use the NG string to analyze the interaction potential and scattering amplitude in the Regge limit ($s \gg -t \sim \Lambda_{\rm QCD}^2$), between two QCD dipoles using the exchange of a NG string in flat 4-dimensional space, without recourse to holography. When formulated in Euclidean signature, the two calculations parallel each other with the scattering following from the potential with an Euclidean-angle valued rotation, followed by a pertinent analytical continuation to the hyperbolic angle or rapidity. This construction was initially suggested for a pair of quark scattering in [15]. For completeness, we recall that this stringy approach to scattering in QCD, was initially proposed in higher dimensions using the gauge-gravity duality [16–18], and since then discussed by many e.g., [19–22] (and references therein).

The present work relies on preceding constructions [23,24], to derive a number of new results: 1) The static dipole-dipole potential is dominated by the exchange of NG closed strings, with the tachyon dominant at large distances; 2) The NG exchanges are characterized by an emergent entropy, that undergoes a phaselike transition with varying separation; 3) The scattering of two dipoles at large rapidity, is dominated by the two-particle irreducible (2PI) NG surface of genus 2, with a total cross section that is in good agreement with the recently reported data at the LHC; 4) The NG estimate of the rapidity and parton-x at saturation; 5) The contribution of the NG world sheet fermions to both the Pomeron intercept, and quantum entanglement at low parton-x; 6) A new entanglement entropy for multiple NG exchanges in the process of shadowing, that asymptotes a single qubit at the Froissart bound; 7) The generalization of the NG tachyon diffusion from flat to curved hyperbolic and confining space, to include evolution in the size of the probing dipoles.

The organization of the paper is as follows: In Sec. II we detail the construction of the potential between two static dipoles of fixed and equal size, via the exchange of closed NG strings. The potential is found to be attractive at all separations, with the NG tachyon dominant at large separations. In Sec. III we extend the potential analysis to the scattering amplitude, through a simple rotation in Euclidean signature, followed by an analytical continuation to rapidity in Minkowski signature. The NG tachyon is shown to dominate the scattering amplitude at large rapidities. Both the potential and scattering amplitude exponentiate through 2PI "webs" that are identified with the exchange of a NG string, in leading order in $1/N_c$. This resummation in the scattering channel, yields to saturation of the total cross section by quantum shadowing, even though the string bits density keeps increasing exponentially at large rapidities. In Sec. IV we review and extend the string results for quantum entanglement for hadron-hadron in the Regge limit, and deep inelastic scattering (DIS) in the low-x regime. We suggest that the quantum entanglement entropy saturates at the Froissart bound. In Sec. V we show how to extend the NG tachyon diffusion in curved transverse space, by including the size of the probe dipoles and enforcing conformal symmetry. The result is reminiscent of the Balitsky-Fadin-Kuraev-Lipatov (BFKL) evolution result following from Mueller's wavefunction evolution for the total cross section in perturbative QCD. Our conclusions are in Sec. VI. A short parallel between the NG tachyon results and pQCD in the Regge limit, is discussed in the Appendix.

II. STRINGY DIPOLE-DIPOLE INTERACTION

There are many indications from lattice simulations that flux tubes in quenched QCD, can be described by an effective theory of strings of which the NG action is the leading contribution [2]. Remarkably, the NG string appears to describe remarkably well the fuzzy QCD string, even for relatively short distances. We now use this lattice observation, to analyze the potential between a pair of static dipoles, in quenched QCD. This potential is amenable to a measurement on the lattice.

This construction parallels closely the analysis of the scattering of a pair of lightlike dipoles discussed in [23] (and references therein), using the holographic construction. To our knowledge, the potential between two parallel

dipoles was never analyzed using the holographic string. It cannot be deduced from the twisted dipoles in [23] by taking the twisting angle to zero, since the twisted exchange presents an essential singularity in this limit. The singularity reflects on the existence of a pair creation process through a string-like Schwinger mechanism in the twisted configuration, that is absent in the untwisted configuration for the potential analysis.

A. Dipole-dipole correlator

Consider the static correlators of two identical Wilson loops

$$\mathbf{WW} = \frac{\langle \mathbf{W}(a, \mathbf{b}_\perp)\mathbf{W}(a, \mathbf{0}_\perp)\rangle}{\langle \mathbf{W}\rangle\langle \mathbf{W}\rangle}, \tag{2}$$

with

$$\mathbf{W}(a, \mathbf{x}_\perp) = \frac{1}{N_c}\mathrm{Tr}\left(\mathbf{P}\exp\left(ig_Y\int_{\mathcal{C}_a} d\tau \mathbf{A}.\mathbf{v}\right)\right). \tag{3}$$

The contour $\mathcal{C}_a$ runs along the rectangular loop of side a, located at $\mathbf{x}_\perp$, with infinite extent along the temporal direction in the v-direction. As usual, the Wilson-loop correlator exponentiates through 2PI "webs" [25,26], which we identify to leading order as a closed NG string with genus 2. More specifically,

$$\ln \mathbf{WW} \equiv \mathbf{WW}_{\mathrm{2PI}} = g_s^2\int \frac{dT}{2T}\mathbf{K}(T), \tag{4}$$

with $g_s \sim \frac{1}{N_c}$ the string coupling, and

$$\mathbf{K}(T) = \int_T D[x]e^{-S[x]+\mathrm{ghost}}, \tag{5}$$

the NG string partition function with cylindrical topology and modulus T. The NG action in conformal gauge is [27]

$$S[x] = \frac{\sigma_T}{2}\int_0^T d\tau\int_0^1 d\sigma(\dot{x}^\mu\dot{x}_\mu + x'^\mu x'_\mu). \tag{6}$$

Here $\dot{x} = \partial_\tau x$ and $x' = \partial_\sigma x$. The string tension is $\sigma_T = 1/(2\pi\alpha')$.

The evaluation of (4) in string theory, is in general difficult due to the finite dipole sizes, and we need to make reasonable approximations. For small size dipoles, we will assume that the cylindrical boundaries are highly pinched, and approximate them by straight lines. The exchanged closed string forms a funnel, with linear end-points, much like the exchange between static $D0$ branes, as detailed for the twisted dipoles in [23]. However, funnels with higher windings or N-ality are not suppressed between $D0$ branes, but are suppressed between dipoles of finite transverse size. A physical interpretation of the final result, will allow for a simple extraction of the dipole-dipole potential from this approximation below.

B. Static dipole-dipole potential

With this in mind, we now decompose the string embedding coordinates using the world sheet normal modes in $2 + D_\perp$ flat space, with linear and periodic boundary conditions in the affine time with period T [28],

$$\begin{aligned}
x^0(\tau,\sigma) &= X + \frac{cW}{\sigma_T}\tau + \sum_{m=-\infty}^{\infty}\sum_{n=1}^{\infty} x^0_{m,n}\exp\left(i2\pi m\frac{\tau}{T}\right)\cos(\pi n\sigma),\\
x^1(\tau,\sigma) &= \sum_{m=-\infty}^{\infty}\sum_{n=1}^{\infty} x^1_{m,n}\exp\left(i2\pi m\frac{\tau}{T}\right)\sin(\pi n\sigma),\\
x_\perp(\tau,\sigma) &= \left(\sigma-\frac{1}{2}\right)b_\perp + \sum_{m=-\infty}^{\infty}\sum_{n=1}^{\infty} x^\perp_{m,n}\exp\left(i2\pi m\frac{\tau}{T}\right)\sin(\pi n\sigma),
\end{aligned} \tag{7}$$

with $c = 1/l_s$. Since

$$x^0(\tau+T,\sigma) - x^0(\tau,\sigma) = W\left(\frac{T}{\sigma_T l_s}\right), \tag{8}$$

we interpret $W = 0, \pm1, \pm2, \ldots$ as a winding number, with $2\pi l_s T$ the circumference of the cylindrical funnel. Below we will show that this is at the origin of an effective temperature for the exchanged closed strings, in the dipole-dipole potential. X, W plays the role of collective coordinates.

In terms of (7), all integrals in (5) are Gaussian with the result

$$\begin{aligned}
\int dX\sum_W \mathbf{K}(T,W) = \frac{a^2X}{l_s^3}\sum_W \exp\left(-\frac{T}{2}\left[\sigma_T b^2 + \frac{c^2W^2}{\sigma_T T^2}\right]\right)\\
\times\left[\prod_{n=1}^{\infty} 2\sinh\left(\frac{n\pi T}{2}\right)\right]^{-D_\perp}.
\end{aligned} \tag{9}$$

The diverging products can be regularized by standard zeta function regularization, using the representation

$$\sinh(\pi x) = \pi x \prod_{m=1}^{\infty}\left(1+\frac{x^2}{m^2}\right). \tag{10}$$

With this in mind, and trading the re-summation over the windings using the Poisson summation formula, we obtain

$$\int dX \sum_W \mathbf{K}(T,W) = \sqrt{\frac{1}{c^2\alpha' T}}\frac{a^2 X}{l_s^3}\sum_k \exp\left(-\frac{T}{2}\left[\sigma_T b^2 + \frac{2\pi k^2}{c^2\alpha' T^2}\right]\right)\eta^{-D_\perp}\left(i\frac{T}{2}\right), \tag{11}$$

where $\eta(x)$ is Dedekind eta function

$$\eta(\tau) = q^{\frac{1}{24}}\prod_{n=1}^{\infty}(1-q^n) \quad q = e^{2i\pi\tau}. \tag{12}$$

Note that (12) satisfies $\eta(ix) = \eta(i/x)/\sqrt{x}$, and relates to the string density of modes [29]

$$\eta^{-D_\perp}(ix) = x^{\frac{D_\perp}{2}} e^{\frac{\pi D_\perp}{12x}} \sum_{n=0}^{\infty} d(n) e^{-n\frac{2\pi}{x}}, \tag{13}$$

with $d(n)$ being the string density of states normalized to $d(0)=1$, with asymptotically

$$d(n) \approx C n^{-\frac{D_\perp+3}{4}} e^{2\pi\sqrt{D_\perp n/6}}. \tag{14}$$

The Poisson resummation trades the sum over the windings W of the closed string exchanges, with the dual sum over the N-alities or k fluxes [23]. For source dipoles as Wilson loops in the fundamental representation, $k = 1,\ldots,[\frac{N_c}{2}]$ which runs to infinity in the large N_c limit. For QCD with $[\frac{3}{2}]=1$, only the $k=1$ N-ality is to be retained.

The leading contribution to the static potential for two parallel dipoles of size a, is given by the 2-particle irreducible (2PI) string exchange

$$V_{DD}(b) = -\frac{\ln \mathbf{WW}}{X} = -g_0^2 \sum_{n=0}^{\infty} d(n)\Delta(m_n, b) \tag{15}$$

with the exchanged scalar propagator

$$\Delta(m_n,b) = \int \frac{dk^{D_\perp+1}}{(2\pi)^{D_\perp+1}}\frac{e^{ik\cdot b}}{k^2+m_n^2} = \frac{1}{2\pi}\left(\frac{m_n}{2\pi b}\right)^{\frac{D_\perp-1}{2}} K_{\frac{D_\perp-1}{2}}(m_n b) \tag{16}$$

and coupling to the dipole $g_0 = \frac{g_s a}{\alpha'}(\sqrt{2\pi}\alpha')^{\frac{D_\perp}{4}}$. Here $\mathbf{K}_\alpha(x)$ is the modified Bessel function, and $d(n)$ is the canonical string density of states with $d(0)=1$, and g_s the string coupling. (15) amounts to a tower of closed string exchanges or glueballs, with radial masses

$$m_n = \frac{1}{c\alpha'}\left(1-\frac{D_\perp c^2}{12\pi\sigma_T}+\frac{2n\pi c^2}{\pi^2\sigma_T}\right)^{\frac{1}{2}} = \sigma_T\beta\left(1-\frac{\beta_H^2}{\beta^2}+\frac{8\pi n}{\sigma_T\beta^2}\right)^{\frac{1}{2}}, \tag{17}$$

and with the inverse Hagedorn temperature $\beta_H = \sqrt{\pi D_\perp/3\sigma_T}$. $\beta = 2\pi/c = 2\pi l_s$ is the circumference of the exchanged cylindrical world sheet.

For large b, the exchange in (15) is dominated by the tachyon mode with $n=0$

$$m_0 = \sigma_T\beta\left(1-\frac{\beta_H^2}{\beta^2}\right)^{\frac{1}{2}} = \frac{1}{l_s}\left(1-\frac{D_\perp}{6}\right)^{\frac{1}{2}}, \tag{18}$$

which is still real positive for $D_\perp < 6$. For $D_\perp = 2$ and using half the rho meson Regge slope $\alpha' = 1/4m_\rho^2$ for a closed string, we have $m_0 \approx 1257$ MeV, which is close to the $m_{0^{++}} = 1475$ MeV glueball reported on the lattice [30]. The attractive and static dipole-dipole potential follows as

$$V_{DD}(b) \approx -\frac{g_s^2 a^2\sqrt{\pi\sigma_T}}{\alpha'}\left(\frac{\pi\alpha' m_0}{b}\right)^{\frac{D_\perp-1}{2}} \mathbf{K}_{\frac{D_\perp-1}{2}}(m_0 b). \tag{19}$$

For short separations, the exchange is also attractive

$$V_{DD}(b) \approx -\left(\frac{g_s^2 a^2\sqrt{\pi\sigma_T}}{2\alpha'}\sum_n d(n)\right)\Gamma\left(\frac{D_\perp-1}{2}\right)\times\left(\frac{1}{\sigma_T b^2}\right)^{\frac{D_\perp-1}{2}}, \tag{20}$$

and Coulombic for $D_\perp = 2$, i.e., $V_{DD}(b) \sim -g_s^2/b$. However, this contribution signals the onset of a critical NG string, with a diverging mode sum for the overall coefficient. At short separations, the exchange is not confining. It is dominated by 2-gluon Coulomb exchange in the 0^{++} channel. The Casimir-Polder contribution characterizes the fully nonconfining potential at large separations [31] (and references therein).

Recall that the string coupling is $g_s = f(\lambda)/N_c$, with $f(\lambda)$ a nonuniversal function of the large 't Hooft coupling $\lambda = g_Y^2 N_c$. For instance, in holographic models, $f(\lambda) = \lambda/4\pi$ ($\mathcal{N}=4$ SUSY) and $f(\lambda) = (\lambda/3)^{\frac{3}{2}}/\pi$ (Witten model). This observation shows that the 2-PI contribution (15) is dominant in large N_c, as the higher #-PI contributions are suppressed by $(1/N_c^2)^{1+\#}$.

C. Emergent entropy in dipole-dipole interaction

The circumference $\beta = 2\pi l_s$ in (15), plays the role of an inverse effective temperature, associated with the spatial

exchange of closed strings or glueballs, in the transverse b-direction. Remarkably, $T_R = 1/\beta = 1/2\pi l_s$ is identical to the Rindler temperature of falling matter on the stretched horizon, a membrane a string length away from the event horizon of a stationary black hole. With this in mind, we may interpret the potential in (15) as a free energy. As a result, the stringy exchange in the dipole-dipole potential, carries an emergent entropy,

$$S_{EV}(b) = \beta^2\left(\frac{\partial V_{DD}(b)}{\partial\beta}\right). \tag{21}$$

To understand the nature of this entropy and how it may relate to the spatial entanglement entropy in QCD_4 at large N_c, we note that (15) at large separation is given by

$$V_{DD}(b) \sim \sqrt{\frac{\pi}{2}}\left(\frac{g_s^2a^2}{\alpha'^{\frac{3}{2}}}\right)\left(\frac{2\pi\alpha'}{b^2}\right)^{\frac{D_\perp-1}{2}}\sum_{n=0}^{\infty} d(n)x_n^{\frac{D_\perp}{2}-1}e^{-x_n} \tag{22}$$

with $\alpha' = l_s^2$ and $x_n = m_n b$. Inserting (22) in (21) gives

$$S_{EV}(b) \sim (2\pi)^{\frac{D_\perp}{2}+4}\left(\frac{g_s^2a^2}{2b^2}\right)\left(\frac{l_s}{b}\right)^{D_\perp-1}\sum_{n=0}^{\infty} d(n)x_n^{\frac{D_\perp}{2}-2}e^{-x_n}. \tag{23}$$

Equation (23) amounts to the entropic function at large $x_n \gg 1$,

$$C_{DD}(b) = \frac{\partial S_{EV}(b)}{\partial \ln b} \sim -(2\pi)^{\frac{D_\perp}{2}+4}\left(\frac{g_s^2a^2}{2b^2}\right) \times \left(\frac{l_s}{b}\right)^{D_\perp-1}\sum_{n=0}^{\infty} d(n)x_n^{\frac{D_\perp}{2}-1}e^{-x_n}. \tag{24}$$

Using the radial mass spectrum (17) and the string density of states (14), the sum is dominated by the large-n contribution

$$\sum_{n=0}^{\infty} d(n)x_n^{\frac{D_\perp}{2}-1}e^{-x_n} \sim \int_{n_{\rm low}}^{\infty} dn n^{-\frac{5}{4}}e^{-m_n b+2\pi\sqrt{\frac{D_\perp n}{6}}}. \tag{25}$$

Using the change of variable $t = \sqrt{8\pi n/\sigma_T}/\beta$ we can rewrite (25) as

$$\int_{t_{\rm low}}^{\infty}\frac{dt}{t^{\frac{3}{2}}}e^{\frac{1}{2}\sigma_T\beta\beta_H t-\sigma_T\beta b\sqrt{1+t^2}}, \tag{26}$$

which can be undone by saddle point approximation for $\beta/b \ll 1$, with the result,

$$\sum_{n=0}^{\infty} d(n)x_n^{\frac{D_\perp}{2}-1}e^{-x_n} \sim e^{-\sigma_T b\sqrt{b^2-(\beta_H/2)^2}}, \tag{27}$$

to exponential accuracy. The branch point singularity $b = \frac{1}{2}\beta_H = R_c$ reflects on the diverging sum for small distances in agreement with (2).

We now recall that the entropic function for spatial entanglement in QCD4 at large N_c, was argued to be of the form [32]

$$C_{1+3}(b) \sim \frac{1}{32\sqrt{\pi}}\frac{V_2}{b^2}\sum_{n=0}^{\infty} d(n)(M_n b)^{\frac{3}{2}}e^{-2M_n b} \sim \int^{\infty} dM M^{\alpha}e^{(\beta_H-2b)M}, \tag{28}$$

where $M_n \sim \sqrt{n}/\alpha'$ was used for the asymptotic of the glueball spectrum. If instead, the exact radial glueball spectrum (17) with $M_n = \frac{1}{2}m_n$ which carries the same asymptotics is used in (25), then to exponential accuracy in the entropic function for spatial entanglement in QCD4

$$\sum_{n=0}^{\infty} d(n)(M_n b)^{\frac{3}{2}}e^{-2M_n b} \sim e^{-\sigma_T b\sqrt{b^2-(\beta_H/2)^2}} \tag{29}$$

in agreement with (27).

We conclude that the entropic function constructed from the emergent entropy (21) associated to two interacting dipoles, shares the same asymptotic behavior as the entropic function for spatial entanglement in QCD4 at large N_c. It also diverges at the same location $b = \frac{1}{2}\beta_H$. The divergence reflects on the transition from a confining to a deconfining phase as probed by (21) and similarly by (29). Amusingly, the mode sums in both cases are identical for $D_\perp = 5$ or a NG in $(2+5)$-dimensions, which is somehow reminiscent of the holographic proposal.

III. STRINGY DIPOLE-DIPOLE SCATTERING

At large center-of-mass energy with a large rapidity gap, the hadron-hadron scattering amplitude is universal. The amplitude is that of two fixed-size dipoles scattering elastically. For small angle scattering, the amplitude is dominated by gluon exchanges with vacuum quantum numbers. In perturbative QCD, the exchange is captured by the BFKL resummation of rapidity ordered gluons, the so-called hard Pomeron. In nonperturbative QCD, the resummation is captured by Reggeized gluons. In the planar approximation, the exchange is stringlike with the topology of a cylinder, the so-called soft Pomeron. The existence of a hard and soft Pomeron at large rapidity, was initially pointed out in [33]. It finds a natural description in the gravity dual approach to QCD [19,20], using a critical string in ten dimensions in the conformal limit (hard Pomeron), followed by conformal symmetry breaking (soft Pomeron).

The purpose of this section is to show that the NG string which is noncritical, allows for the description of the elastic dipole-dipole scattering amplitude using $1/N_c$ counting

rules, already in four dimensions. The result is a soft Pomeron with parameters that are distinct from the holographic results. The scattering construction parallels that of the dipole-dipole interaction, showing the interconnectedness of the potential and scattering problems. The hard Pomeron can also be retrieved, by allowing the tachyon mode in the NG string to diffuse both in transverse and longitudinal size, a point inspired by holography [24]. Since the NG string provides the closest description of the QCD string potential, it should prove relevant for the QCD scattering amplitude in the eikonal limit. In particular, a more transparent approach to the unitarization of the cross section, as well as the partonic string bit content and entanglement, are seen to emerge.

The present construction using a NG string in $D=4$ dimensions is the closest to the holographic construction using $D>4$ presented in [23,24], with an essential difference in the Pomeron intercept. The twisted dipole-dipole correlator follows from the reduction of the eikonal QCD scattering amplitude, and then evaluated using the closed and noncritical NG string in flat $D=4$ dimensions. The exchange is solely in the confining regime of QCD. It differs from the holographic Pomeron discussed in [19], by the value of its intercept, the coupling to the sourcing dipoles, and the absence of a conformal limit. This can remedied as we discuss below.

A. Scattering amplitude

In Euclidean signature, the scattering between two dipoles follows the same analysis as that for the potential between two static dipoles presented above, with one difference; the dipoles are not parallel but slated at an angle θ. This angle maps by analytical continuation to the rapidity or boost angle χ, thanks to Minkowski historical observation. With this in mind, a rerun of the preceding arguments gives for the twisted world sheet propagator [23]

$$\mathbf{K}(T,\theta)=\frac{a^2}{\alpha'}\frac{e^{-\frac{\sigma_T}{2}Tb^2}}{2\sinh\left(\frac{\theta T}{2}\right)}\prod_{n=1}^{\infty}\prod_{s=\pm}\frac{\sinh\left(\frac{n\pi T}{2}\right)}{\sinh\left[\frac{T(n\pi+s\theta)}{2}\right]}\times\left[\prod_{n=1}^{\infty}2\sinh\left(\frac{n\pi T}{2}\right)\right]^{-D_\perp}. \tag{30}$$

The details regarding the twisted string world sheet mode decomposition analogous to (7), followed by the detailed mode integration leading to (30) are given in [23]. The double analytical continuation $T\to iT$ and $\theta\to -i\chi$, maps this twisted dipole-dipole correlator onto the scattering amplitude of two light-like Wilson loops. With this in mind, inserting (30) in the corresponding **WW** 2PI correlator and using (12), (13), yield [23]

$$\begin{aligned}\mathbf{WW}_{\rm 2PI}(\chi,a,b)&=\frac{g_s^2a^2}{4\alpha'}\sum_{k=1}^{\infty}\frac{(-1)^k}{k}e^{-k\frac{\pi\sigma_T\mathbf{b}^2}{\chi}}\eta^{-D_\perp}\left(\frac{ik\pi}{\chi}\right)\\&=\frac{g_s^2a^2}{4\alpha'}\sum_{k=1}^{\infty}\sum_{n=0}^{\infty}d(n)\frac{(-1)^k}{k}\left(\frac{k\pi}{\chi}\right)^{\frac{D_\perp}{2}}\\&\quad\times\exp\left(-\frac{2\chi}{k}\left[n+\frac{\mathbf{b}^2}{\alpha'(2\chi/k)^2}-\frac{D_\perp}{24}\right]\right),\end{aligned} \tag{31}$$

after analytical continuation, with $\chi\approx\ln(\alpha' s)$ identified as the rapidity, for large invariant mass $\sqrt{s}$. The scattering amplitude in momentum space is

$$\begin{aligned}\frac{1}{-2is}\mathcal{T}_{DD}(\chi,q)&\approx\int d^2\mathbf{b}e^{i\mathbf{q}_\perp\cdot\mathbf{b}}\mathbf{WW}_{\rm 2PI}(\chi,a,b)\\&\approx\frac{\pi^2g_s^2a^2}{2}\sum_{n=0}^{\infty}\sum_{k=1}^{\infty}d(n)\frac{(-1)^k}{k}\left(\frac{k\pi}{\chi}\right)^{\frac{D_\perp-2}{2}}\\&\quad\times\exp\left(-\frac{2\chi}{k}\left[n+\frac{\alpha'}{4}\mathbf{q}_\perp^2-\frac{D_\perp}{24}\right]\right).\end{aligned} \tag{32}$$

Again, k sums over the N-ality with $k=1,\ldots,[\frac{N_c}{2}]$ all the way to infinity at large N_c. In our case, only the $k=1$ term contributes to the scattering of two dipoles as twisted Wilson loops, in the fundamental representation of $SU(3_c)$. With this in mind, and in the large rapidity limit, (32) simplifies

$$\mathcal{T}_{DD}(\chi,q)\approx is(\pi g_s a)^2\left(\frac{\pi}{\chi}\right)^{\frac{D_\perp}{2}-1}\exp\left(-\chi\left[\frac{\alpha'}{2}(\mathbf{q}_\perp^2+M_0^2)\right]\right), \tag{33}$$

with the tachyon squared mass $M_0^2=-\frac{D_\perp}{6\alpha'}$.

The closed string exchange amounts to a Pomeron exchange, with a Regge trajectory

$$\alpha_{\mathbb{P}}(t)=\frac{D_\perp}{12}+\frac{\alpha'}{2}t, \tag{34}$$

hence a dipole-dipole (hadron-hadron) scattering amplitude that rises as $\sigma_{\mathbb{P}}(s)\sim s^{\alpha_{\mathbb{P}}(t)}$. In the Regge limit with $-t\ll s$, this amplitude is dominated by a single NG string exchange, given by

$$\mathcal{A}(s,t)\sim -2is\int d^2b e^{iq\cdot b}\mathbf{WW}_{\rm 2PI}(s,a,b)\sim is^{1+\alpha_{\mathbb{P}}(t)}, \tag{35}$$

with $t=-q^2$.

B. Cross section and Froissart bound

The elastic-scattering amplitude (36) yields the total cross section

$$\sigma(s)=\frac{1}{s}\mathrm{Im}\mathcal{A}(s,0)\sim -2\int d^2b\mathbf{WW}_{\mathrm{2PI}}(s,a,b)\sim s^{\alpha_{\mathbb{P}}(0)}, \tag{36}$$

by the optical theorem. (36) increases with the squared invariant mass s, in violation of unitarity. This shortcoming can be addressed by noting that $\langle\mathbf{WW}\rangle$ as a correlator of two Wilson loops, requires the exponentiation of all the 2PI contributions in leading order in $\frac{1}{N_c}$, much like in the potential between the two static dipoles discussed earlier

$$\begin{aligned}\mathbf{WW}(\chi,a,b)&=\frac{\langle\mathbf{W}_{\frac{\chi}{2}}(a,\mathbf{b}_\perp)\mathbf{W}_{-\frac{\chi}{2}}(a,\mathbf{0}_\perp)\rangle}{\langle\mathbf{W}\rangle\langle\mathbf{W}\rangle}\\&=\exp[\mathbf{WW}_{\mathrm{2PI}}(\chi,a,b)].\end{aligned} \tag{37}$$

$\mathbf{WW}_{\mathrm{2PI}}$ is the 2PI "web" contributions [25,26], which is dominated by a string exchange with genus 2 as detailed above, with higher genus contributions suppressed by powers of $g_s^2\sim 1/N_c^2$. Since $\mathbf{WW}\equiv\mathcal{S}$ identifies with the full S-matrix, and using $\mathcal{S}=1+i\mathcal{T}$ as detailed in Appendix, we obtain

$$\begin{aligned}\sigma(s)&=2\int d^2b\mathrm{Re}(1-\mathcal{S}(\chi,a,b))\\&=2\int d^2b(1-e^{\mathbf{WW}_{\mathrm{2PI}}(\chi,a,b)}),\end{aligned} \tag{38}$$

since $\mathbf{WW}_{\mathrm{2PI}}(\chi,a,b)$ is real. To proceed, it is useful to recast the tachyon contribution in (31) in impact parameter space, as follows [23]:

$$\mathbf{WW}_{\mathrm{2PI}}(\chi,a,b)\approx-\frac{g_s^2a^2}{4\alpha'}\left(\frac{\pi}{\chi}\right)^{\frac{D_\perp}{2}}e^{-S_{\mathrm{cl}}-S_{\mathrm{1loop}}}. \tag{39}$$

The first contribution in the exponent of (39)

$$S_{\mathrm{cl}}=\sigma_T\int_0^{T_P}\cos^2(\chi\tau)bd\tau\int_0^1 bd\sigma=\frac{1}{2}\sigma_T\beta b=\frac{b^2}{2\alpha'\chi}, \tag{40}$$

is identified with a semiclassical world sheet instanton, with a tunneling time $T_P=1/\beta=2\pi b/\chi$. The second contribution in the exponent of (39)

$$S_{\mathrm{1loop}}=\frac{D_\perp}{2}\ln\det(-\partial_\perp^2)=-\frac{\pi D_\perp}{6}\frac{b}{\beta}=-\frac{D_\perp}{12}\chi, \tag{41}$$

is the 1-loop zeta regulated corrective action, around the world sheet instanton.

Using (39)–(41), we now note that the integrand in (38) is controlled by the exponent in (31), which is a tradeoff between the minimal world sheet instanton action S_{cl} and its 1-loop quantum correction S_{1loop}. The black disc radius is reached when

$$S_{\mathrm{cl}}=|S_{\mathrm{1loop}}|\to b_{\max}^2=\frac{D_\perp\alpha'}{6}\chi^2, \tag{42}$$

so that $e^{\mathbf{WW}_{\mathrm{2PI}}}\to\theta(b-b_{\max})$. As a result (38) yields the total cross section

$$\sigma(s)\sim 2\int d^2b\theta(b_{\max}-b)\sim 2\pi b_{\max}^2=2\pi\alpha'\frac{D_\perp\chi^2}{6}. \tag{43}$$

At large rapidity, the 2PI NG contribution saturates the Froissart bound, with a scale fixed by the string tension $\sigma_T=1/2\pi\alpha'$, and not the pion mass as suggested in [23,34,35].

More specifically, (38) evaluates exactly to

$$\begin{aligned}\sigma(s)=2\pi\alpha'\Bigg(&\frac{D_\perp\chi^2}{6}-\chi\ln(D_\perp\chi)+\left(\frac{a^2g_s^2\pi}{4\alpha'}\chi+\gamma_E\right)\\&+\mathcal{O}\left(e^{-\frac{a^2g_s^2\pi}{4\alpha'\chi}e^{\frac{D_\perp\chi}{6}}}\right)\Bigg),\end{aligned} \tag{44}$$

with $\chi=\ln(\alpha's)$, in agreement with the estimate (43). The new result (44) stemming from the NG exchange, is to be compared with the empirical parametrization of the pp data by the COMPETE Collaboration [12]

$$\sigma^{pp}(s)\sim\left(35.5+0.307\ln^2\left(\frac{s}{29.1\ \mathrm{GeV}^2}\right)\right)\ \mathrm{mb}, \tag{45}$$

after dropping the Reggeon contributions at large $\sqrt{s}$. In Fig. 1 we show the NG result for the total cross section (44) for $a=l_s$ and $g_s=1$ with $\mathcal{O}=30$: green-solid upper curve with $\alpha'=l_s^2=1/2m_\rho^2$ (the rho meson trajectory slope), and red-solid curve with $\alpha'=l_s^2=1/4m_\rho^2$ (half the rho meson

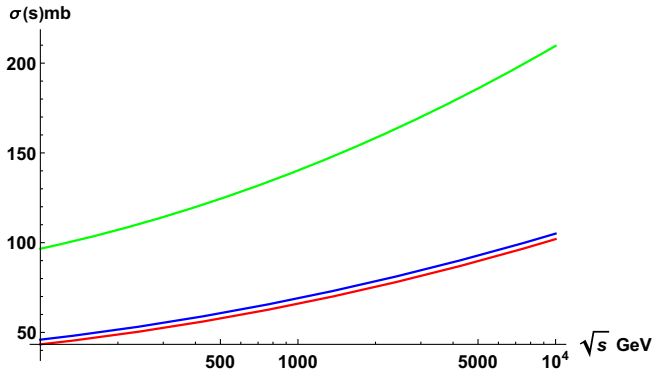

FIG. 1. Total cross section in mb versus $\sqrt{s}$ in GeV: solid-red lower curve is the empirical pp cross section as parametrized by the COMPETE Collaboration in [12] and quoted in (45). It is in agreement with the cross sections currently measured by the LHC [13]. The solid-blue lower curve is the NG result (44) with $a=l_s$ and $g_s=1$ and $\mathcal{O}=30$, with $\alpha'=1/4m_\rho^2$, while the solid-green upper curve is for $\alpha'=1/2m_\rho^2$.

trajectory slope). The empirical parametrization (45) blue-solid lower curve, has been used by the COMPETE Collaboration to reproduce the compiled pp and $p\bar{p}$ data, two decades ago. It is in good agreement with the recently reported TOTEM measurements for pp at the highest $\sqrt{s} = 13$ TeV at the LHC [13]. The NG result is mostly sensitive to the string length, and is undistinguishable from the COMPETE parametrization for $\alpha' = l_s^2 = 1/4m_\rho^2$. Note that the value of this parameter is tied to glueball spectrum in (18). This shows the duality between the scattering amplitude of two dipoles, and the static potential between two dipoles.

C. Shadowing of wee string bits

We now note that the total cross section (38) amounts to

$$\sigma(s) \sim 2 \int d^2b N(s,a,b), \tag{46}$$

with

$$\frac{1}{2}\frac{d\sigma}{d^2b} = N(s,a,b) = 1 - S(s,a,b) = 1 - e^{\mathbf{WW}_{2\mathrm{PI}}(s,a,b)}, \tag{47}$$

and $\frac{1}{2}$ the effective number of wee-string bits flowing through the cylindrical annulus $2\pi b db$. The effective number N, obeys a nonlinear diffusionlike equation

$$(\partial_\xi + M_0^2 - \nabla_\perp^2)\ln(1-N) = 0, \tag{48}$$

with $\xi = \frac{1}{2}\alpha'\chi$ playing the role of an effective (Gribov) time, or

$$\partial_\xi N - M_0^2(1-N)\ln(1-N) - \nabla_\perp^2 N - \frac{(\nabla_\perp N)^2}{1-N} = 0. \tag{49}$$

In the small number limit $\ln(1-N) \sim -N$, one recovers the linear diffusion equation, with nonlinear corrections for larger N, that cause saturation asymptotically. For instance, in the quadratic approximation, the nonlinear evolution is given by

$$(\partial_\xi + M_0^2 - \nabla_\perp^2)N - \frac{M_0^2}{2}N^2 - (\nabla_\perp N)^2 + \mathcal{O}(N^3) = 0, \tag{50}$$

which is reminiscent of the nonlinear Gribov-Levin-Ryskin equation, for the unintegrated gluon distribution [36].

In Fig. 2 we show the behavior of the integrand in the total cross section (46) versus the rapidity, for three different values of the impact parameter b. The green-solid upper curve, red-solid middle curve, and the blue-solid lower curve are for impact parameters $b = 2, 4, 6$, in units of the string length. We have set the string coupling $g_s = 1$, and the static dipole sizes $a = 1$ in units of the string length. The dependence on the impact parameter is mild.

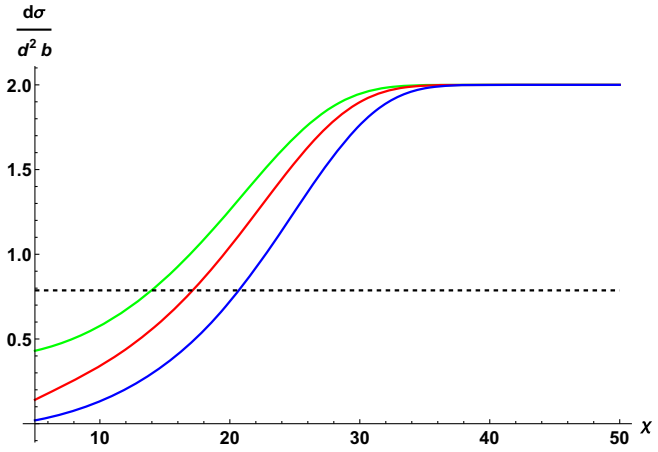

FIG. 2. Differential cross section (46) for fixed impact parameter b between two dipoles of fixed size $a = 1$ and $g_s = 1$, as it unitarizes by shadowing, at large rapidity χ. The green-solid upper curve, red-solid middle curve, and the blue-solid lower curve are for impact parameters $b = 2, 4, 6$, in units of the string length. The dashed line follows from the saturation condition (55).

D. Deep inelastic scattering view of wee-string bits

In the stringy approach to the Pomeron and unitarization, the picture of a hadron at large rapidities or small x, is different from that following from pQCD, where a hadron at large rapidity χ preserves its transverse size, and shrinks its longitudinal size by the gamma factor $\gamma = e^{\frac{1}{2}\chi}$. In contrast, when a string is exchanged, the hadron transverse size grows logarithmically as $|\Delta x_\perp| \sim \sqrt{\chi\alpha'}$, while its light front longitudinal size grows parametrically as $|\Delta x^-| \sim \chi^0\alpha'/0^+$, with 0^+ the time resolution in the light front coordinate x^+ [14] (note that $\Delta x^- \Delta x^+ \sim \alpha'$ by the uncertainty principle). Parton as wee-string bits do not behave as normal matter under Lorentz boost.

The number of wee-string bits grows exponentially with $\mathbf{WW}_{2\mathrm{PI}} \sim e^{\alpha_{\mathbb{P}}\chi}$. This growth is similar to the growth of the longitudinal light front momentum $P^+ \sim \gamma \sim e^{\frac{1}{2}\chi}$, of the boosted hadron. The string growth persists, even though the total cross section saturates by quantum shadowing, with $\rho(\chi)$ the number of string bits per light front volume $|\Delta x_\perp||\Delta x^-|$,

$$\textbf{diffusive regime}: \; b_\perp \sim \sqrt{\alpha'\chi} \quad \rho(\chi) \sim \frac{e^{\alpha_{\mathbb{P}}\chi}}{\chi\alpha'^2/0^+},$$
$$\textbf{ballistic regime}: \; b_\perp \sim \sqrt{\alpha'}\chi \quad \rho(\chi) \sim \frac{1}{\chi^2\alpha'^2/0^+}. \tag{51}$$

An illustration of this spatial growth under boosting of the nucleon is shown in Fig. 3. The ballistic regime dominates the total cross section.

These features are accessible to DIS scattering at large $Q^2/m_H^2 \gg 1$ and small parton faction $x \ll 1$, where the virtual photon can be viewed as a small projectile dipole of

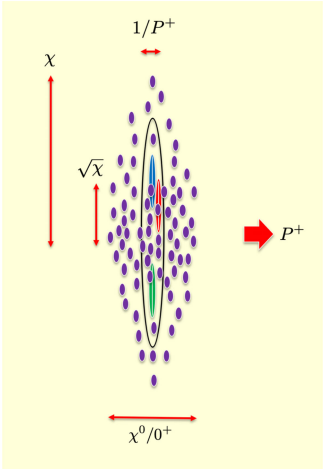

FIG. 3. Boosted nucleon with large longitudinal momentum $P^+ \sim e^{\frac{1}{2}\chi}$. The confined quark-diquark pair is highly contracted, with a vanishingly small longitudinal size $1/P^+$, and fixed transverse size χ^0. It is surrounded by a halo of partons as string bits, which extends transversely as $\sqrt{\chi}$ (diffusive regime) and up to χ (ballistic regime). The halo remains parametrically large longitudinally as $\chi^0/0^+$, with 0^+ the time resolution along x^+ [14]. Throughout, it is described by a continuous NG string with longitudinal momentum P^+. All dimensions are in string units.

size $a_P \sim 1/\sqrt{Q^2}$, scattering off a target hadron also as a dipole of a larger size a_T, as illustrated in Fig. 4. We recall the DIS kinematics

$$s - m_H^2 = Q^2\left(\frac{1}{x} - 1\right)$$

with the identification $\chi \to \ln\frac{1}{x}$. For a fixed target size, (39) translates to

$$\mathbf{WW}_{\mathrm{2PI}}(Q^2, x, b) \sim g_s^2 \frac{1}{\sqrt{\alpha' Q^2}} \frac{1}{x^{\alpha_{\mathbb{P}}(0)}} e^{-\frac{\mathbf{b}_\perp^2}{2\alpha' \ln\frac{1}{x}}} \sim \left(\frac{Q^2(x)}{Q^2}\right)^{\frac{1}{2}} e^{-\frac{\mathbf{b}_\perp^2}{2\alpha' \ln\frac{1}{x}}}, \tag{52}$$

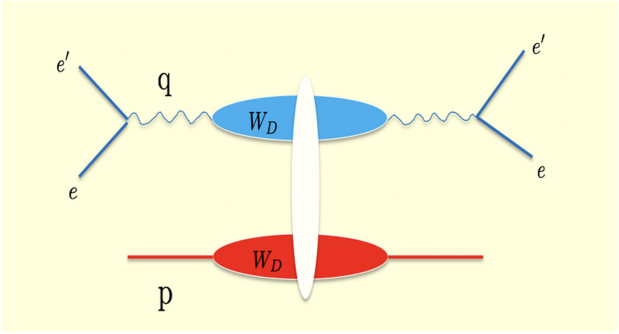

FIG. 4. DIS scattering as two Wilson loops $\mathbf{W}_D$ exchanging a closed NG string, in the Regge limit.

after re-insertion of the preexponent, with

$$Q(x) = \frac{g_s^2}{\sqrt{\alpha'}} \frac{1}{x^{\alpha_{\mathbb{P}}(0)}}. \tag{53}$$

The arguments presented in Appendix show that the F_2 structure function is

$$F_2(x, Q^2) \sim x G_{\mathbb{P}}(x, Q^2) \sim \left(\frac{Q^2(x)}{Q^2}\right)^{\frac{1}{2}}, \tag{54}$$

at low-x, where $Q(x)$ maybe regarded as the stringy analog of the so-called saturation momentum, with differences with the original proposal by Golec-Biernat-Wusthoff (GBF) [37]. The standard condition for saturation is set by the requirement that $S(s, a, b)|_S = e^{-\frac{1}{2}}$ in (47) (a drop by one standard deviation in the GBF Gaussian proposal for S), or equivalently

$$\left.\frac{d\sigma}{d^2b}\right|_S = 2\left(1 - e^{-\frac{1}{2}}\right) = 0.79 \;\to\; 14 < \chi_S = \ln\frac{1}{x_S} < 20. \tag{55}$$

The rightmost result follows numerically from the black-dashed curve in Fig. 2, for the impact parameter b in the range $2 < b/l_s < 6$. This stringy estimate puts a lower bound on parton x at saturation $x_S > 10^{-6}$, which falls outside the reach of current colliders, including the future EIC. This conclusion is specific to the Pomeron as the exchange of noncritical NG string in $D = 4$ dimensions.

Finally, (52) may be viewed as the number of wee string bits with parton x, at a distance $b_\perp = \sqrt{\mathbf{b}_\perp^2}$ in the transverse plane, surrounding a fast moving hadron sourced by a fixed size dipole. The number is small for $Q^2 \gg Q^2(x)$, whatever $b_\perp$. It is large for $Q^2 \ll Q^2(x)$, only in the disc $b_\perp \sim \sqrt{\alpha' \ln\frac{1}{x}}$, which is seen to grow diffusively in the immediate surrounding of the target dipole. It drops substantially in the much wider corona $b_\perp \sim \sqrt{\alpha'} \ln\frac{1}{x}$, where the growth is ballistic.

IV. ENTANGLEMENT IN SCATTERING

In the large rapidity limit, (31) is dominated by the tachyon contribution in the closed string exchange described by the Nambu-Goto string. The tachyon as a mode encodes the quantum entanglement between the projectile and the target, carried geometrically by the world sheet. A way to quantify this, is to recast (31) in the form (41). This is readily identified as the free energy of $D_\perp$ massless bosons trapped in a box of size b at temperature $1/\beta$ as illustrated in Fig. 5, with [38]

$$S_{1\mathrm{loop}} = \beta F_B = D_\perp \int \frac{bdp}{2\pi} \ln(1 - e^{-\beta|p|}). \tag{56}$$

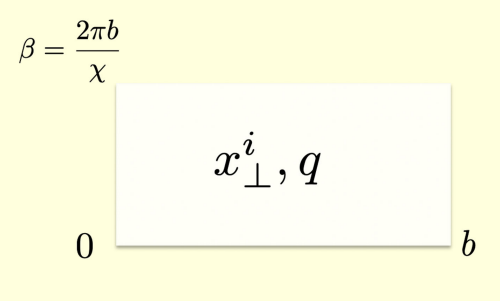

FIG. 5. String world sheet exchange $\beta \times b$ in the Regge limit. The transverse fluctuations $x^i_\perp$ with $i = 1, \ldots, D_\perp$, and the n_f massless fermions q, are subject to periodic boundary conditions in β.

As a result, the exchange in Fig. 5 carries a quantum or entanglement bosonic entropy

$$S_{EB} = \beta^2 \frac{\partial F_B}{\partial \beta} = D_\perp \int \frac{bdp}{2\pi} \frac{2\beta|p|}{e^{\beta|p|} - 1} = \frac{D_\perp}{6}\chi = 2\alpha_{\mathbb{P}}(0)\chi. \tag{57}$$

Equation (57) clearly captures the entropy of fluctuating string bits (gluonic dipoles) on the instanton world sheet of size $\beta \times b$.

A. Fermionic contribution to the Pomeron intercept and deep inelastic scattering

The fermionic correction to (57) follows immediately from this physical observation, as n_f massless world sheet fermions also trapped in $\beta \times b$ as illustrated in Fig. 5, with the result

$$\beta F_F = n_f \int \frac{bdp}{2\pi} \ln(1 + e^{-\beta|p|}), \tag{58}$$

in total analogy with (56). The corresponding quantum or entanglement fermionic entropy is then

$$S_{EF} = \beta^2 \frac{\partial F_F}{\partial \beta} = n_f \int \frac{bdp}{2\pi} \frac{2\beta|p|}{e^{\beta|p|} + 1} = \frac{1}{2}\frac{n_f}{6}\chi, \tag{59}$$

with a net entanglement entropy

$$S_{EE} = S_{EB} + S_{EF} = \left(1 + \frac{1}{2}\frac{n_f}{D_\perp}\right)\frac{D_\perp}{6}\chi. \tag{60}$$

The result (60) implies that the stringy Pomeron intercept is affected by the fermionic corrections on the world sheet. More specifically, the Pomeron contribution in hadron-hadron scattering is modified, with a shifted intercept

$$\alpha_{\mathbb{P}}(t) = \frac{D_\perp}{12} + \frac{\alpha'}{2}t \to \tilde{\alpha}_{\mathbb{P}}(t) = \left(1 + \frac{1}{2}\frac{n_f}{D_\perp}\right)\frac{D_\perp}{12} + \frac{\alpha'}{2}t, \tag{61}$$

due to the fermionic contribution.

Also in DIS, we can reinterpret the gluonic F_2 structure function (54) at low x as

$$F_2(x, Q^2) \sim xG_{\mathbb{P}}(x, Q^2) \sim \frac{1}{x^{\tilde{\alpha}_{\mathbb{P}(0)}}}, \tag{62}$$

at the resolution fixed by the probing dipole size $Q \sim 1/a$. Note that (60) is still solely given by the gluon density (62) at low x

$$S_{EE}(x, Q^2) \sim \ln(xG_{\mathbb{P}}(x, Q^2)), \tag{63}$$

albeit with a fermion corrected gluonic intercept. At low x, the partonic evolution does not follow from Dokshizer-Gribov-Lipatov-Altarelli-Parisi equations (DGLAP), but rather BFKL (weak coupling) or surfaces (strong coupling). An alternative proposal to account for the fermionic contribution to the entanglement entropy at low x was suggested in [39–41].

B. Entanglement and Froissart bound

Finally, we suggest that in Reggeized hadron-hadron scattering at the Froissart bound, the entanglement entropy saturates by quantum shadowing, even though the entanglement entropy as measured by (63) in DIS does not. For that, we interpret the 2PI stringy exchanges in the shadowing process in (38), as a net-quantum free energy

$$F_{2\text{PI}} = -\frac{1}{\beta}\ln(2(1 - e^{\mathbf{WW}_{2\text{PI}}})). \tag{64}$$

Note that it reduces to the stringy free energy for small $\mathbf{WW}_{2\text{PI}}$ and large rapidity. Hence the 2PI quantum or entanglement entropy

$$S_{2\text{PI}} = \beta^2 \frac{\partial F_{2\text{PI}}}{\partial \beta} = \ln(1 - e^{\mathbf{WW}_{2\text{PI}}}) + \beta \frac{\partial_\beta \mathbf{WW}_{2\text{PI}}}{1 - e^{-\mathbf{WW}_{2\text{PI}}}} + \ln 2 \to \ln 2, \tag{65}$$

which is seen to asymptote a constant for fixed b and large rapidity $\chi \gg 1$. In the unitarity limit, the entanglement is that of a single qubit! Recall that in the black disc limit, the scattering choice appears to be binary, as the elastic and inelastic cross sections are equal to the classical cross section (Babinet theorem).

In Fig. 6 we show the entanglement entropy versus rapidity, using our proposal (64) for the 2PI contribution, for different values of the impact parameter b. The green-solid lower curve, red-solid middle curve, and blue-solid upper curve, are for impact parameters $b = 2, 4, 6$ and fixed dipole size $a = 1$, all units of the string length. We have

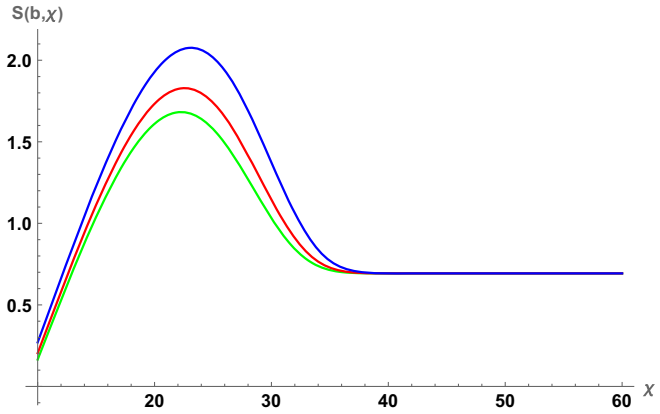

FIG. 6. The entanglement entropy between two light-light scattering dipoles in the Regge limit, versus the rapidity χ, following from the 2PI NG string contribution to the total cross section shown in Fig. 6. The green-solid lower curve, red-solid middle curve, and blue-solid upper are for impact parameters $b = 2, 4, 6$, for a pair of dipoles of fixed size $a = 1$, in units of the string length. The rapid and linear rise in the entanglement entropy with rapidity, is stopped and reversed by quantum shadowing. It levels off asymptotically when the Froissart bound is reached.

fixed the string coupling $g_s = 1$. The rapid initial rise with rapidity, is caused by the NG tachyon in the single-string exchange (60). This rise overshoots the unitarity line, before it is overtaken by quantum shadowing in (65), to level off at the Froissart bound. This leveling off is generic of chaotic systems in their approach to equilibrium [38,42], although here from above and not below.

V. NG TACHYON DIFFUSION IN A CONFINING WARPED SPACE

The scattering amplitude of two fixed dipoles of size a in (33), is dominated by the exchange of the NG tachyon

$$\exp\left(-\chi\left[\frac{\alpha'}{2}(\mathbf{q}_\perp^2 + M_0^2)\right]\right), \tag{66}$$

in the transverse $D_\perp$ dimensions, where the rapidity χ emerges as a proper time. This exchange is diffusive, and can be recast (66) using the contour integral

$$\int_{-i\infty}^{+i\infty}\frac{dj}{2i\pi}\frac{e^{\chi j}}{j+\frac{\alpha'}{2}(M_0^2+\mathbf{q}_\perp^2)} = \frac{2}{\alpha'}\int_{-i\infty}^{+i\infty}\frac{dj}{2i\pi}e^{\chi j}G(j,\mathbf{q}_\perp). \tag{67}$$

The propagator in the complex j-plane satisfies

$$(\mathbf{q}_\perp^2 + m_j^2)G(j,\mathbf{q}_\perp) = 1, \tag{68}$$

with the j-dependent mass $m_j^2 = \frac{2}{\alpha'}(j - j_0)$ and $j_0 = \frac{D_\perp}{12}$. This stringy result captures the exchange of an emergent spin-j in the Regge limit, for fixed momentum transfer $\mathbf{q}_\perp$, sourced by a projectile and a target dipole of fixed sizes (both set to a).

A. Warped diffusion

In QCD a boosted hadron is a collection of wee dipole of various sizes as we discussed earlier. The scattering between these dipoles is mediated by a noncritical NG string. Large-size wee dipoles scattering mostly in the IR, through the exchange of a closed NG string in the confining regime. Small size dipoles scatter mostly in the conformal regime, albeit at strong coupling in our case. The chief results are different transverse growth size of the string, at the origin of the transverse size dependence of the saturation scale: 1) in the confining regime the growth is linear in the root of the rapidity as in (52); 2) in the conformal regime, the growth is exponential in the rapidity as we show below.

With this in mind, the sourcing dipole sizes vary as well, with the combined change in $a, b_\perp$, expected to be conformal in the UV, and stringy in the IR. To realize this, we rewrite (68) in a general coordinate space

$$-\frac{1}{\sqrt{|g|}}\partial_\mu(\sqrt{|g|}g^{\mu\nu}\partial_\nu G) + m_j^2 G = \frac{1}{\sqrt{|g|}}\delta(z-z')\delta^{D-1}(\vec{x}-\vec{x}'), \tag{69}$$

by combining $(a, \mathbf{b}_\perp) \to (z, \vec{x}) = x^\mu$ in $D = 1 + D_\perp$ space. But what is the metric $g_{\mu\nu}$ when z is added as a coordinate? (69) can be viewed as an evolution equation in our QCD analysis of the scattering amplitude, with the evolution taking place in $z \sim 1/\sqrt{Q^2}$ and rapidity χ. Hence, the metric should exhibit conformal symmetry for small z. Inspired by holography, we fix $g_{\mu\nu}$ through the line element

$$ds^2 = \frac{R^2}{z^2}e^{\mp\kappa^2 z^2}(dz^2 + d^2x_\perp). \tag{70}$$

For small size dipoles $z \to 0$, (70) reduces to that of AdS_3 which is conformal. For large size dipoles $z \to 1/\kappa$ as expected from confinement for both warping signs. Although (70) is reminiscent of the holographic analysis of the Pomeron in $AdS_5 \times S_5$ [19], we emphasise that the present construction is not holographic. The starting point is the NG string in flat space with a tachyon for $D_\perp = 2$, with no reference to type-IIB string theory in 10-dimensions with no tachyon [1] (and references therein). As we noted earlier, the NG string in 4-dimension is the only effective string model currently supported by QCD lattice simulations. We define

$$\frac{R^2}{\alpha'} \equiv \sqrt{\lambda}, \tag{71}$$

with κ, R to be tied below. Since our approach is not holographic, the identification $\lambda = g_Y^2 N_c$ does not follow. However, it is natural to expect that $R/l_s \gg 1$, since R is the radius of the hyperbolic space, where the warped evolution of the NG tachyon is justified for large transverse separations.

With this in mind, and using (70) in (69), we obtain

$$-\partial_z^2 G(z,z',t) + (D-2)\left(\frac{1}{z} \pm \kappa^2 z\right)\partial_z G(z,z',t) + \left(t + \frac{S}{z^2} e^{\mp \kappa^2 z^2}\right) G(z,z',t) = z^{D-2} e^{\pm(\frac{D}{2}-1)\kappa^2 z^2}\delta(z-z'), \tag{72}$$

with $\partial_\perp^2 \to t$ and

$$S \equiv S_j = 2\sqrt{\lambda}(j - j_0). \tag{73}$$

To remove the first order derivative, we redefine

$$G(z,z',t) \to z^{\frac{D-2}{2}} e^{\pm\frac{D-2}{4}\kappa^2 z^2} z'^{\frac{D-2}{2}} e^{\pm\frac{D-2}{4}\kappa^2 z'^2} G(z,z',t), \tag{74}$$

set $u = \kappa z$, expand $e^{\mp u^2} = 1 \mp u^2 + \mathcal{O}(u^4)$ (moderately small size dipoles) to obtain

$$-\frac{d^2}{du^2} G(u,u',t) + \left(\frac{S_j + \frac{D(D-2)}{4}}{u^2} + \frac{u^2}{4}(D-2)^2 + \frac{t}{\kappa^2} \mp S_j \pm \frac{1}{2}(D-2)(D-3)\right) G(u,u',t) = \delta(u-u'). \tag{75}$$

For $D = 1 + D_\perp = 3$, we have explicitly

$$-\frac{d^2}{du^2} G(u,u',t) + \left(\frac{S_j + \frac{3}{4}}{u^2} + \frac{u^2}{4} + \frac{t}{\kappa^2} \mp S_j\right) G(u,u',t) = \delta(u-u'). \tag{76}$$

B. Repulsive warping

The repulsive warping with $e^{+\kappa^2 z^2}$ acts as absolute confinement for the dipole sizes in hyperbolic space, characterizing the evolution. (In holography, it is a regulated hard wall in bulk AdS). In this case the linear and homogeneous equation (76) becomes

$$-\frac{d^2}{du^2} G(u) + \left(\frac{S + \frac{D(D-2)}{4}}{u^2} + \frac{u^2}{4}(D-2)^2 + \frac{t}{\kappa^2} + S - \frac{1}{2}(D-2)(D-3)\right) G(u) = 0. \tag{77}$$

To simplify the equation, we consider $u \to u' = \sqrt{D-2}u = \sqrt{D-2}\kappa z$, for which (77) reads

$$-\frac{d^2}{du^2} G(u) + \left(\frac{S + \frac{D(D-2)}{4}}{u^2} + \frac{u^2}{4} + \tilde{t} + \tilde{S} - \frac{1}{2}(D-3)\right) G(u) = 0. \tag{78}$$

With

$$D_\perp = D - 1, \qquad \tilde{t} = \frac{t}{(D-2)\kappa^2}, \qquad \tilde{S} = \frac{S}{D-2}, \tag{79}$$

the general solutions are of the form

$$G_1(u) = e^{-\frac{u^2}{4}} u^{1+\sqrt{\frac{D_\perp^2}{4} + (D_\perp - 1)\tilde{S}}} \mathbb{M}\left(\frac{2 - \frac{D_\perp}{2} + \tilde{S} + \tilde{t} + \sqrt{\frac{D_\perp^2}{4} + (D_\perp - 1)\tilde{S}}}{2}, 1 + \sqrt{\frac{D_\perp^2}{4} + (D_\perp - 1)\tilde{S}}, \frac{u^2}{2}\right),$$
$$G_2(u) = e^{-\frac{u^2}{4}} u^{1+\sqrt{\frac{D_\perp^2}{4} + (D_\perp - 1)\tilde{S}}} \mathbb{U}\left(\frac{2 - \frac{D_\perp}{2} + S + \tilde{t} + \sqrt{\frac{D_\perp^2}{4} + (D_\perp - 1)\tilde{S}}}{2}, 1 + \sqrt{\frac{D_\perp^2}{4} + (D_\perp - 1)\tilde{S}}, \frac{u^2}{2}\right), \tag{80}$$

where $\mathbb{M}(a,b,z)$ and $\mathbb{U}(a,b,z)$ are the Kummer $\mathbb{M}$ function and the Tricomi $\mathbb{U}$ function, respectively. $\mathbb{M}$ is regular at $u = 0$, while $\mathbb{U}$ has a branch cut at $u = 0$. The solution to (76) reads

$$G(u,u') = \mathcal{A} G_2(u) G_1(u') \quad u > u',$$
$$G(u,u') = \mathcal{A} G_1(u) G_2(u') \quad u < u', \tag{81}$$

with $\mathcal{A}^{-1}$ given by the Wronskian

$$\mathcal{A} = \frac{1}{\mathcal{W}(G_1, G_2)} \sim -\Gamma\left(\frac{2 - \frac{D_\perp}{2} + \tilde{t} + \tilde{S} + \sqrt{(D_\perp - 1)\tilde{S} + \frac{D_\perp^2}{4}}}{2}\right). \tag{82}$$

C. Reggeized trajectories

$\mathcal{A}$ has poles when

$$\frac{\tilde{t}+\tilde{S}+2-\frac{D_\perp}{2}+\sqrt{(D_\perp-1)\tilde{S}+\frac{D_\perp^2}{4}}}{2}=-n \tag{83}$$

or squared masses $|t(j,n)|$ given by

$$|\tilde{t}(j,n)|=2n+\tilde{S}+2-\frac{D_\perp}{2}+\sqrt{(D_\perp-1)\tilde{S}+\frac{D_\perp^2}{4}}. \tag{84}$$

By extending the tachyon diffusion to AdS_3 space, the original tachyon pole morphs into a multitude of Regge poles,

$$\tilde{S}=\frac{2\sqrt{\lambda}(j-j_0)}{D_\perp-1}=\frac{-5+2D_\perp-4n+\frac{2|t|}{(D_\perp-1)\kappa^2}\pm\sqrt{(2D_\perp-3)^2-8(D_\perp-1)n+\frac{4|t|}{\kappa^2}}}{2}. \tag{85}$$

For $n=0$ and small t, the Regge trajectories for the $\pm$ signs are

$$\begin{aligned} j_+&=j_0+\frac{(D_\perp-1)(D_\perp-2)}{\sqrt{\lambda}}+\left(\frac{3D_\perp-4}{D_\perp-2}\right)\frac{\alpha'}{2}|t|+\mathcal{O}(t^2)\\ j_-&=j_0-\frac{D_\perp-1}{2\sqrt{\lambda}}+\frac{\alpha'}{2}|t|+\mathcal{O}(t^2) \end{aligned} \tag{86}$$

provided that

$$\kappa^2R^2=\frac{D_\perp-2}{2D_\perp-3}$$

with $\sqrt{\lambda}=R^2/\alpha'$. The dominant contribution to the Pomeron stems from the j_- trajectory, which is the closest to the origin in the j-plane. The warping shifts down the flat space intercept j_0.

D. Confining regime

For large t and large n the poles in the j-plane become imaginary, but with negative real parts. To proceed with the contour integration in (67) for the tachyon propagator, we select the branch cut of $\sqrt{S+1}$ from $-1-i\infty$ to -1. With this in mind, the dominant contribution stems from the first pole $n=0$ with $j=j_-$. At the pole, the hypergeometric functions in (80) simplify

$$\begin{aligned} &\mathbb{M}\left(0,1+\sqrt{S+\frac{D_\perp^2}{4}},\frac{u^2}{2}\right)=1,\\ &\mathbb{U}\left(0,1+\sqrt{S+\frac{D_\perp^2}{4}},\frac{u^2}{2}\right)=1. \end{aligned} \tag{87}$$

Using (80), (81), and (87) in (67) and carrying the j-integral gives the warped tachyon propagator

$$G(z,z',b_\perp)\sim(zz')^{D_\perp-\frac{1}{2}}\int\frac{d^2q}{(2\pi)^2}e^{\chi(j_0-\frac{D_\perp-1}{2\sqrt{\lambda}}-\frac{\alpha' q^2}{2})+iq\cdot b} \tag{88}$$

after rewinding the redefinition (74), for large χ. The result for the warped tachyon propagator is

$$G(z,z',b_\perp)\sim(zz')^{D_\perp-\frac{1}{2}}e^{\chi(j_0-\frac{D_\perp-1}{2\sqrt{\lambda}})-\frac{b_\perp^2}{2\chi\alpha'}} \tag{89}$$

(89) reduces to the unwarped result with a shifted down intercept.

E. Conformal regime

The effects of the warping is mostly in action away from the confining regime. Indeed, in the conformal regime, the hypergeometric functions are limited to small $u=\kappa z$ and large $t\gg\kappa^2$, which we will refer to as the conformal limit. More specifically, this amounts to the limits

$$\lim_{\kappa\to0}G_1(u),\qquad G_2(u), \tag{90}$$

which are not simply the $u\to0$ limits, because $\frac{t}{\kappa^2}$ in the second argument has to go to infinity. To obtain these limits, the simplest way is to note that the differential equation (78) reduces to

$$-\frac{d^2}{dz^2}G(z)+\left(\frac{S+\frac{D(D-2)}{4}}{z^2}+t\right)G(z)=0, \tag{91}$$

with two solutions

$$\tilde{G}_1(z)=\sqrt{z}J_{-\sqrt{S+\frac{D_\perp^2}{4}}}(-i\sqrt{t}z), \tag{92}$$

$$\tilde{G}_2(z)=\sqrt{z}Y_{-\sqrt{S+\frac{D_\perp^2}{4}}}(-i\sqrt{t}z). \tag{93}$$

Here $-\sqrt{S+\frac{D_\perp^2}{4}}$ is chosen to have a negative real part. With this in mind, the warped tachyon propagator in the conformal limit is of the form

$$G(z,z',b_\perp)=\frac{\pi t}{2}\sqrt{zz'}J_{-\sqrt{S+\frac{D_\perp^2}{4}}}(-i\sqrt{t}z_<)Y_{-\sqrt{S+\frac{D_\perp^2}{4}}}(-i\sqrt{t}z_>). \tag{94}$$

For $b_\perp \gg z,z'$, the Bessel functions reduce to

$$J_{-\sqrt{S+\frac{D_\perp^2}{4}}}(-i\sqrt{t}z)\to\frac{1}{\Gamma(1-\sqrt{S+\frac{D_\perp^2}{4}})}\left(\frac{\sqrt{t}z}{2}\right)^{-\sqrt{S+\frac{D_\perp^2}{4}}}, \tag{95}$$

$$Y_{-\sqrt{S+\frac{D_\perp^2}{4}}}(-i\sqrt{t}z_>)\to\cos\left(\pi\sqrt{S+\frac{D_\perp^2}{4}}\right)\Gamma\left(\sqrt{S+\frac{D_\perp^2}{4}}\right)\left(\frac{\sqrt{t}z}{2}\right)^{-\sqrt{S+\frac{D_\perp^2}{4}}}. \tag{96}$$

As a result, the warped tachyon propagator in the conformal regime is dominated by the following S integral

$$G(z,z',b_\perp)\sim\int\frac{d^2q}{(2\pi)^2}e^{iq\cdot n_\perp}\int dS\exp\left(\chi\left(j_0+\frac{S}{2\sqrt{\lambda}}\right)+\left(\frac{1}{2}-\sqrt{\frac{D_\perp^2}{4}+S}\right)\ln\left(\frac{zz'q^2}{2b_\perp^2}\right)\right), \tag{97}$$

with $n_\perp$ a unit vector along $q_\perp$ after rescaling away the transverse momentum, and trading $j\to\tilde{S}$ using (79). The result is

$$G(z,z',b_\perp)\sim\frac{\xi}{(4\pi\mathcal{D}\chi)^{\frac{3}{2}}}\exp\left(\chi\left(j_0-\frac{\mathcal{D}D_\perp^2}{4}\right)-\frac{\xi^2}{4\chi\mathcal{D}}\right), \tag{98}$$

with the conformal variable $\xi=\ln\frac{b_\perp^2}{zz'}$ and diffusion like constant $\mathcal{D}=\frac{1}{2\sqrt{\lambda}}$.

F. Cross section in conformal regime

In terms of (98), the dipole-dipole scattering amplitude in the conformal regime is now

$$\mathbf{WW}_{\mathrm{2PI}}=-\frac{g_s^2}{4}(2\pi)^{\frac{3}{2}}G=-\frac{g_s^2\xi}{4(2\mathcal{D}\chi)^{\frac{2}{3}}}e^{\tilde{j}_0\chi-\frac{\xi^2}{4\chi\mathcal{D}}}, \tag{99}$$

with $\tilde{j}_0=j_0-\frac{1}{4}\mathcal{D}D_\perp^2$. Inserting (99) in the 2PI contribution to the total cross section (38) gives

$$\begin{aligned}\sigma(s)&=2\int d^2b(1-e^{\mathbf{WW}_{\mathrm{2PI}}})\\&=2\pi zz'\int_0^\infty d\xi e^\xi\left(1-\exp\left(-\frac{g_s^2\xi}{4(2\mathcal{D}\chi)^{\frac{2}{3}}}e^{\tilde{j}_0\chi-\frac{\xi^2}{4\chi\mathcal{D}}}\right)\right).\end{aligned} \tag{100}$$

For $\tilde{j}_0<4\mathcal{D}$, the integral in (100) can be undone for large χ, with the result for the total cross section in the conformal regime

$$\sigma(s)\to 2\pi zz'\frac{g_s^2\sqrt{\pi}}{2\sqrt{2}}e^{\chi\left(j_0-\mathcal{D}\left(\frac{D_\perp^2}{4}-1\right)\right)}. \tag{101}$$

It grows exponentially, i.e., $\sigma(s)\sim zz's^{j_0}$ with $j_0=\frac{D_\perp}{12}=\frac{1}{6}$ for $D_\perp=2$, much like the BFKL result in pQCD, which is also conformal at weak coupling.

Modulo the NG string assignments for j_0 and $\mathcal{D}$, the contribution (98) to the Reggeized scattering amplitude, and the total dipole-dipole cross section, is analogous to the result following from Mueller's dipole wave function evolution in pQCD [43]. More importantly, the results (89) (confining regime) and (98) (conformal regime), show that the general and warped NG result (80) interpolates continuously between these two regimes in Reggeized scattering. This point was originally made in the context of the gravity dual construction [19,20], with no tachyon in bulk.

VI. CONCLUSIONS

One of the most striking features of the detailed lattice studies of the fuzzy QCD string, is its description as a fundamental NG string for large and even relatively small lengths. This observation has been numerically checked in both 3- and 4-dimensions, and for different SU(N_c) realizations. We have used this observation, to analyze

the stringy potential between a pair of static and scattering dipoles, as well as their quantum entanglement.

The derivation of the static potential of two fixed-size dipoles, follows from the exchange of closed strings or glueballs in the quenched approximation (large N_c limit). Using the NG string, we have shown that this exchange is dominated by the tachyonic mode and attractive at large distances. The attraction persists at short distances, albeit in a power law form following from the resummation over the string states. This change in the static potential is captured by an emergent quantum entropy.

The derivation of the scattering amplitude for two fixed-size dipoles can be obtained using similar arguments, by noting that it follows from a potential between two dipoles set at an angle θ, which is then analytically continued to the rapidity $i\chi$. In the Regge limit, the scattering amplitude is totally fixed by the tachyonic mode of the NG string, as all the excited modes are suppressed at large rapidity. There is a total parallel between the potential channel and the scattering channel, where the 2PI contribution is retained in both, in leading order in $1/N_c$. This contribution yields unitarization by saturation of the Froissart bound.

We have extended some results regarding the quantum entanglement as captured by the NG tachyon in dipole-dipole scattering. The inclusion of the world sheet fermions, modify the intercept of the stringy Pomeron, thereby changing the quantum entanglement as measured by DIS through solely a modification of the gluonic density. In the presence of shadowing, the quantum entanglement entropy is depleted, and saturates at the Froissart bound.

The NG tachyon contribution to the Reggeized scattering amplitude of two dipoles, captures two key aspects of the exchanged string: (1) an exponential growth in the number of string bits at the origin of the growth of the total cross section at large rapidity prior to saturation; (2) a diffusive spread of the string bits in the transverse plane. It is the balance between these two phenomena that yields saturation by quantum shadowing, as captured by the 2PI contribution.

Perturbative QCD arguments using BFKL evolution of gluons as dipoles, have shown that the gluon sizes evolve and that the evolution is conformal in the UV. This aspect of QCD in the Regge limit, can be extended to the exchanged NG string, by considering the diffusive spreading of the string bits in the transverse plane together with the changes in the source and target dipole sizes. In other words, the NG tachyonic mode should diffuse in conformal 3-dimensional space (transverse space plus dipole size) as opposed to simply 2-dimensional space (transverse space).

We have shown how to explicitly extend the diffusion of the NG tachyon mode in flat transverse space, to curved AdS_3 plus a repulsive wall. We have emphasized that this approach is not holographic, since no string-gauge duality is used. In the conformal limit, the modified NG tachyon diffusion in proper time and curved space, yields results for the scattering amplitude of two dipoles with evolving sizes, similar to those following from the BFKL evolution of Mueller's wave function in QCD. In the confining regime, the NG tachyon diffusion is preserved, albeit with a shifted down intercept.

ACKNOWLEDGMENTS

We thank Krzysztof Kutak for discussions. This work is supported by the Office of Science, U.S. Department of Energy under Contract No. DE-FG-88ER40388 and by the Priority Research Areas SciMat and DigiWorld under program Excellence Initiative—Research University at the Jagiellonian University in Kraków.

APPENDIX: RELATION TO pQCD DIPOLES

There are few parallels between the stringy results we have developed, and those established using pQCD. In particular, the 2PI string amplitude (38) at fixed b, can be recast in the form

$$1 - e^{\mathbf{WW}(s,a,b)} = 1 - \exp\left(-\frac{g_s^2}{4}\frac{a^2}{\alpha'} x G_{\mathbb{P}}(x, 1/a^2) S(b)\right), \tag{A1}$$

with $g_s = f(\lambda)/N_c$, the Gaussian profile

$$S(b) = \left(\frac{\pi}{\chi}\right)^{\frac{D_\perp}{2}} e^{-S_{\min}} = \left(\frac{\pi}{\chi}\right)^{\frac{D_\perp}{2}} e^{-\frac{b^2}{2\alpha'\chi}}, \tag{A2}$$

and $\chi = \ln\frac{1}{x}$ in DIS. The diffusion of the string bits in the transverse plane is manifest in (A2). (A1) is very similar to the Glauber-Mueller formula for multiple dipole-target interactions [44]

$$N_{\mathrm{GM}}(x_{01}, x, b) = 1 - \exp\left(-\frac{\lambda}{N_c^2}\frac{x_{01}^2}{8R^2} x G_{\mathrm{DGLAP}}(x, 4/x_{01}^2) S(b)\right), \tag{A3}$$

where the dipole size is x_{01} (a in our case), R is the radius of the target (#$\sqrt{\alpha'}$ in our case), and $S(b)$ is identified with the dipole profile function inside the target [(A2) in our case]. Equation (A3) is an extension of the original Golec-Biernat-Wusthoff formula for the analysis of saturation in DIS at HERA [37], through the addition of the profile function.

In general, the forward amplitude $\mathcal{T}(b_\perp, \chi)$ of dipole-nucleus scattering at impact parameter $b_\perp$ and rapidity χ, relates to the full S-matrix $\mathcal{S}(b_\perp, \chi)$ as

$$1-\mathcal{S}(b_\perp,\chi)=-i\mathcal{T}(b_\perp,\chi), \tag{A4}$$

and the total cross section is given by

$$\sigma(\chi)=2\int d^2b\,\mathrm{Re}(1-\mathcal{S}(b_\perp,\chi)). \tag{A5}$$

In our case or in the color glass condensate model (CGC), the full S-matrix is approximated by the Wilson-loop average

$$\mathcal{S}=\frac{1}{N_c}\langle \mathrm{Tr}V_{\vec{x}_0}V^\dagger_{\vec{x}_1}\rangle_{\text{target}}, \tag{A6}$$

with $V_{\vec{x}}$ a Wilson line located at $\vec{x}$. If the target is another Wilson-loop, it simply reduces to the **WW** corrector. In the CGC model, this Wilson-loop average exponentiates [45] (and references therein)

$$\mathcal{S}=\exp\left(-\frac{1}{4}x_\perp^2Q_s^2(b_\perp,Y)\ln\frac{1}{|x_\perp|\Lambda}\right). \tag{A7}$$

Our large $b_\perp$ result cuts off the growth by a delicate balance between the factors $e^{\frac{D_\perp\chi}{12}}$ (growth of the string bits) and $e^{-\frac{b^2}{2\chi\alpha'}}$ (diffusion penalty).

[1] Martin Ammon and Johanna Erdmenger, *Gauge/Gravity Duality: Foundations and Applications* (Cambridge University Press, Cambridge, England, 2015).
[2] Julius Kuti, Lattice QCD and string theory, Proc. Sci. LAT2005 (**2006**) 001.
[3] Andreas Athenodorou, Barak Bringoltz, and Michael Teper, The closed string spectrum of SU(N) gauge theories in $2+1$ dimensions, Phys. Lett. B **656**, 132 (2007).
[4] Andreas Athenodorou, Barak Bringoltz, and Michael Teper, The spectrum of closed loops of fundamental flux in $D=3+1$ SU(N) gauge theories, Proc. Sci. LAT2009 (**2009**) 223.
[5] J. F. Arvis, The exact $q\bar{q}$ potential in nambu string theory, Phys. Lett. **127B**, 106 (1983).
[6] M. Luscher, K. Symanzik, and P. Weisz, Anomalies of the free loop wave equation in the WKB approximation, Nucl. Phys. **B173**, 365 (1980).
[7] Martin Luscher and Peter Weisz, String excitation energies in SU(N) gauge theories beyond the free-string approximation, J. High Energy Phys. 07 (2004) 014.
[8] Bastian B. Brandt, Spectrum of the open QCD flux tube and its effective string description I: 3d static potential in SU(N= 2, 3), J. High Energy Phys. 07 (2017) 008.
[9] Bastian B. Brandt, Revisiting the flux tube spectrum of 3d SU(2) lattice gauge theory, Indian J. Phys. **95**, 1613 (2021).
[10] Ofer Aharony and Matan Field, On the effective theory of long open strings, J. High Energy Phys. 01 (2011) 065.
[11] E. Eichten, K. Gottfried, T. Kinoshita, K. D. Lane, and Tung-Mow Yan, Charmonium: The model, Phys. Rev. D **17**, 3090 (1978); **21**, 313(E) (1980).
[12] J. R. Cudell, V. V. Ezhela, P. Gauron, K. Kang, Yu. V. Kuyanov, S. B. Lugovsky, E. Martynov, B. Nicolescu, E. A. Razuvaev, and N. P. Tkachenko (COMPETE Collaboration), Benchmarks for the forward observables at RHIC, the Tevatron Run II and the LHC, Phys. Rev. Lett. **89**, 201801 (2002).
[13] G. Antchev *et al.* (TOTEM Collaboration), First measurement of elastic, inelastic and total cross-section at $\sqrt{s}=13$ TeV by TOTEM and overview of cross-section data at LHC energies, Eur. Phys. J. C **79**, 103 (2019).
[14] Leonard Susskind, Strings, black holes and Lorentz contraction, Phys. Rev. D **49**, 6606 (1994).
[15] Enrico Meggiolaro, A remark on the high-energy quark quark scattering and the eikonal approximation, Phys. Rev. D **53**, 3835 (1996).
[16] Mannque Rho, Sang-Jin Sin, and Ismail Zahed, Elastic parton-parton scattering from AdS/CFT, Phys. Lett. B **466**, 199 (1999).
[17] R. A. Janik and Robert B. Peschanski, Minimal surfaces and reggeization in the AdS/CFT correspondence, Nucl. Phys. **B586**, 163 (2000).
[18] Joseph Polchinski and Matthew J. Strassler, Hard scattering and gauge/string duality, Phys. Rev. Lett. **88**, 031601 (2002).
[19] Joseph Polchinski and Matthew J. Strassler, Deep inelastic scattering and gauge/string duality, J. High Energy Phys. 05 (2003) 012.
[20] Richard C. Brower, Joseph Polchinski, Matthew J. Strassler, and Chung-I Tan, The pomeron and gauge/string duality, J. High Energy Phys. 12 (2007) 005.
[21] Richard C. Brower, String/gauge duality: (Re)discovering the QCD string in AdS space, Acta Phys. Pol. B **34**, 5927 (2003).
[22] Artur Amorim, Miguel S. Costa, and Matti Järvinen, Regge theory in a holographic dual of QCD in the Veneziano limit, J. High Energy Phys. 07 (2021) 065.
[23] Gokce Basar, Dmitri E. Kharzeev, Ho-Ung Yee, and Ismail Zahed, Holographic pomeron and the Schwinger mechanism, Phys. Rev. D **85**, 105005 (2012).
[24] Alexander Stoffers and Ismail Zahed, Holographic pomeron: Saturation and DIS, Phys. Rev. D **87**, 075023 (2013).
[25] J. G. M. Gatheral, Exponentiation of eikonal cross-sections in nonabelian gauge theories, Phys. Lett. **133B**, 90 (1983).
[26] J. Frenkel and J. C. Taylor, Nonabelian eikonal exponentiation, Nucl. Phys. **B246**, 231 (1984).

[27] Alexander M. Polyakov, Fine structure of strings, Nucl. Phys. **B268**, 406 (1986).
[28] Yachao Qian and Ismail Zahed, A stringy (holographic) pomeron with extrinsic curvature, Phys. Rev. D **92**, 085012 (2015).
[29] S. Fubini, D. Gordon, and G. Veneziano, A general treatment of factorization in dual resonance models, Phys. Lett. B **29**, 679 (1969).
[30] Harvey B. Meyer, Glueball regge trajectories, Other thesis, 2004, arXiv:hep-lat/0508002.
[31] Edward V. Shuryak and Ismail Zahed, Instanton induced effects in QCD high-energy scattering, Phys. Rev. D **62**, 085014 (2000).
[32] Igor R. Klebanov, David Kutasov, and Arvind Murugan, Entanglement as a probe of confinement, Nucl. Phys. **B796**, 274 (2008).
[33] A. Donnachie and P. V. Landshoff, Small x: Two pomerons! Phys. Lett. B **437**, 408 (1998).
[34] Shmuel Nussinov, Is the Froissart bound relevant for the total pp cross section at $s = (14\text{-TeV})^2$?, arXiv:0805.1540.
[35] Dmitri Kharzeev, Edward Shuryak, and Ismail Zahed, Higher order string effects and the properties of the Pomeron, Phys. Rev. D **97**, 016008 (2018).
[36] L. V. Gribov, E. M. Levin, and M. G. Ryskin, Semihard processes in QCD, Phys. Rep. **100**, 1 (1983).
[37] Krzysztof J. Golec-Biernat and M. Wusthoff, Saturation in diffractive deep inelastic scattering, Phys. Rev. D **60**, 114023 (1999).
[38] Yizhuang Liu and Ismail Zahed, Entanglement in Regge scattering using the AdS/CFT correspondence, Phys. Rev. D **100**, 046005 (2019).
[39] Dmitri E. Kharzeev and Eugene Levin, Deep inelastic scattering as a probe of entanglement: Confronting experimental data, Phys. Rev. D **104**, L031503 (2021).
[40] Martin Hentschinski and Krzysztof Kutak, Evidence for the maximally entangled low x proton in deep inelastic scattering from H1 data, Eur. Phys. J. C **82**, 111 (2022).
[41] Martin Hentschinski, Krzysztof Kutak, and Robert Straka, Maximally entangled proton and charged hadron multiplicity in deep inelastic scattering, Eur. Phys. J. C **82**, 1147 (2022).
[42] Vito Latora and Michel Baranger, Kolmogorov-sinai entropy rate versus physical entropy, Phys. Rev. Lett. **82**, 520 (1999).
[43] Alfred H. Mueller, Unitarity and the BFKL pomeron, Nucl. Phys. **B437**, 107 (1995).
[44] Alfred H. Mueller, Small x behavior and parton saturation: A QCD model, Nucl. Phys. **B335**, 115 (1990).
[45] Yuri V. Kovchegov and Eugene Levin, *Quantum Chromodynamics at High Energy*, Cambridge Monographs on Particle Physics, Nuclear Physics and Cosmology Vol. 33 (Cambridge University Press, Cambridge, Engalnd, 2022).